



HAL
open science

Control of Quaternary sea-level changes on gas seeps

Vincent Riboulot, Yannick Thomas, Serge S. Berné, Gwenael Jouet, Antonio Cattaneo

► **To cite this version:**

Vincent Riboulot, Yannick Thomas, Serge S. Berné, Gwenael Jouet, Antonio Cattaneo. Control of Quaternary sea-level changes on gas seeps. *Geophysical Research Letters*, 2014, 41 (14), p. 4970-4977. 10.1002/2014GL060460 . hal-01286371

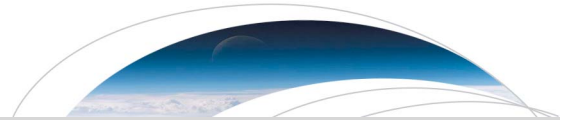
HAL Id: hal-01286371

<https://univ-perp.hal.science/hal-01286371>

Submitted on 10 Mar 2016

HAL is a multi-disciplinary open access archive for the deposit and dissemination of scientific research documents, whether they are published or not. The documents may come from teaching and research institutions in France or abroad, or from public or private research centers.

L'archive ouverte pluridisciplinaire **HAL**, est destinée au dépôt et à la diffusion de documents scientifiques de niveau recherche, publiés ou non, émanant des établissements d'enseignement et de recherche français ou étrangers, des laboratoires publics ou privés.



RESEARCH LETTER

10.1002/2014GL060460

Key Points:

- Pockmarks, in the Gulf of Lions, are associated to oblique gas chimneys
- Evidence of hundreds of pockmarks confined stratigraphically
- Pockmark “life” is governed by Quaternary climate changes

Correspondence to:

V. Riboulot,
riboulot@ifremer.fr

Citation:

Riboulot, V., Y. Thomas, S. Berné, G. Jouet, and A. Cattaneo (2014), Control of Quaternary sea-level changes on gas seeps, *Geophys. Res. Lett.*, *41*, 4970–4977, doi:10.1002/2014GL060460.

Received 13 MAY 2014

Accepted 25 JUN 2014

Accepted article online 27 JUN 2014

Published online 29 JUL 2014

Control of Quaternary sea-level changes on gas seeps

Vincent Riboulot^{1,2}, Yannick Thomas¹, Serge Berné², Gwénaél Jouet¹, and Antonio Cattaneo¹

¹IFREMER, Institut CARNOT—EDROME, REM-GM, Plouzané, France, ²Université de Perpignan Via Domitia, Perpignan, France

Abstract Gas seeping to the seafloor through structures such as pockmarks may contribute significantly to the enrichment of atmospheric greenhouse gases and global warming. Gas seeps in the Gulf of Lions, Western Mediterranean, are cyclical, and pockmark “life” is governed both by sediment accumulation on the continental margin and Quaternary climate changes. Three-dimensional seismic data, correlated to multi-proxy analysis of a deep borehole, have shown that these pockmarks are associated with oblique chimneys. The prograding chimney geometry demonstrates the syn-sedimentary and long-lasting functioning of the gas seeps. Gas chimneys have reworked chronologically constrained stratigraphic units and have functioned episodically, with maximum activity around sea level lowstands. Therefore, we argue that one of the main driving mechanisms responsible for their formation is the variation in hydrostatic pressure driven by relative sea level changes.

1. Introduction

Defined by *King and MacLean* [1970] as sub-circular seafloor depressions, pockmarks result from fluid escape [*Hovland et al.*, 1984] and are commonly associated in depth with a vertical stack of seismic reflection anomalies, such as changes in amplitude, and positive or negative relief. These anomalies, often referred to as “chimneys,” are interpreted as representing both a temporal succession of anomalies along the same migration pathway and a conduit for fluid flow [*Hustoft et al.*, 2007; *Moss and Cartwright*, 2010].

Despite numerous descriptions of pockmarks worldwide, few studies have focused on the mechanisms behind pockmark formation and more particularly on the role of climate changes. Several hypotheses and conceptual models have been proposed by various authors [e.g., *Josenhans et al.*, 1978; *Hovland*, 1987; *Gay*, 2002; *Cartwright et al.*, 2007; *Andresen et al.*, 2008; *Cathles et al.*, 2010; *Agirrezabala et al.*, 2013]. For example, the formation of pockmarks has been explained by catastrophic eruptions of gas from overpressured shallow gas pockets [*Hovland*, 1987], by continuous fluid discharge associated with bottom currents creating sediment fluidization at the seafloor [*Josenhans et al.*, 1978; *Boe et al.*, 1998], and recently by subsidence induced by dewatering and degassing of the gas-charged seafloor, perhaps enhanced by the weight of the carbonate bodies [*Agirrezabala et al.*, 2013]. For 10 years, sea level changes have been suspected to represent a relevant factor in pockmark formation and fluid seepages [*Judd et al.*, 2002; *Rollet et al.*, 2006; *Lafuerza et al.*, 2009; *Hammer and Webb*, 2010; *Andresen and Huuse*, 2011; *Plaza-Faverola et al.*, 2011; *Riboulot et al.*, 2013]. *Rollet et al.* [2006] noticed a relationship between seeps and tidal cycles in which the water column falls by several meters during ebb tides, reducing total water pressure and generating a difference in interstitial pore pressure which allows the expulsion of gas. *Andresen and Huuse* [2011] and *Plaza-Faverola et al.* [2011] have confirmed that sea level fall appears to be the most efficient trigger mechanism for pockmark formation in the Lower Congo Basin and the Nyegga region, respectively. Indeed, *Lafuerza et al.* [2009] and *Riboulot et al.* [2013] have proposed that relative sea level falls decrease hydrostatic pressure and thus increase gas volume in the fluid reservoir, with the formation of gas bubbles subsequently inducing pockmark formation. However, comprehensive detailed scenarios integrating the roles of sedimentation, near-bottom currents, chimney geometry, regional stratigraphic organization, and the timing of pockmark formation remain scarce.

The Bourcart/Hérault (B/H) canyon interfluvial (Figure 1), in the Gulf of Lions (Western Mediterranean), provides one of the most complete data sets available with which to tackle pockmark formation, with the added advantage of a well-constrained chronology [*Sierro et al.*, 2009; *Frigola et al.*, 2012]. The Gulf of Lions is an outstanding zone to understand the impact of sea level on gas seeps because this passive continental margin dominated by subsidence and sediment supply fluctuations derived from glacio-eustatic control is a virtually aseismic zone [*Nocquet*, 2012]. The presence of deep-rooted normal (listric) faults linked to slow

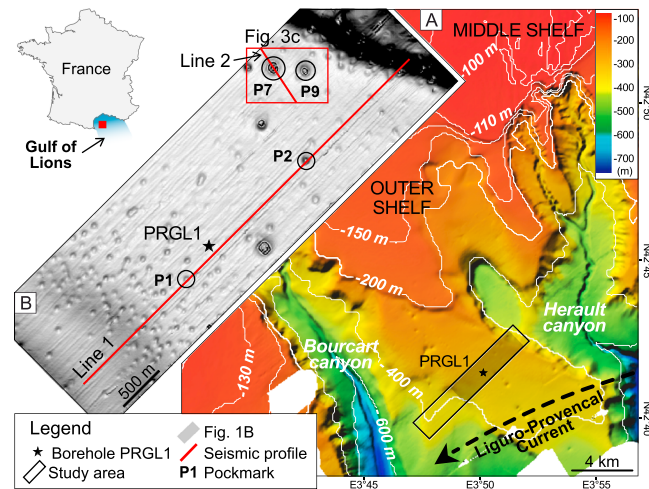


Figure 1. Map of the Bourcart/Hérault canyon interfluvial and pockmark identification in the data set. (a) The study area is located on the upper slope of the Gulf of Lions (GOL), in the vicinity of the Bourcart and Hérault canyons. Present oceanographic circulation is driven by the anticlockwise Liguro-Provençal or Northern Current [Millot, 1990]. (b) Seafloor dip map extracted from 3-D seismic data showing pockmark distribution on the seafloor (location in Figure 1a). P1, P2, P7, and P9 = numbered pockmarks. Lines 1 and 2 = HR seismic profiles extracted from the 3-D seismic block shown in Figures 2 and 3. The red rectangle represents the time slices detailed in Figure 3c.

veneer of biogenic, fine to medium sand forming a condensed deposit, which extends from the inner shelf to the upper slope [Bassetti et al., 2008; Sierro et al., 2009; Frigola et al., 2012]. The PROMESS PRGL1 borehole provides a precise chrono-stratigraphic framework correlated with seismic data [Jouet, 2007; Frigola et al., 2012] and encompassing the last five stratigraphic sequences of the Late Quaternary. Depositional sequences S4 and S5 (upper part of borehole PRGL1) recording the last two 100 kyr climatic cycles are bounded by D50, D60, and D70 that represent Marine Isotope Stages (MIS) 7, 5, and 1, respectively (Figure 2). The average sediment accumulation rate is 0.59 m kyr^{-1} for sequence S5 and 0.35 m kyr^{-1} for sequence S4.

2. Methods

A high-resolution (40–250 Hz) 3-D seismic data set was acquired in 2004 over an $8.5 \times 1.6 \text{ km}$ area of the B/H canyon interfluvial in the Gulf of Lions, surrounding the PROMESS PRGL1 borehole (Figure 1). The seismic layout and 3-D seismic processing sequence [Thomas et al., 2012] provide a lateral resolution of 10 m and a vertical resolution of 2.5 m. Based on this data set, we analyzed (1) the detailed seafloor expression of the pockmarks, (2) the three-dimensional structure of pockmark chimneys, their link with seismic units, and their geometry within each seismic unit. Seismic profiles were processed on a work station, with seismic interpretation and attribute analyses performed using the Kingdom Suite software program. The study of pockmarks associated with an oblique chimney requires the picking of those reflectors marking the tops of the features (Figure 3a). In plan view, the picking of each pockmark on these three discontinuities provides useful information regarding pockmark distribution, which often varies from one sequence to the next (Figure 3b). To analyze the direction of pockmark migration, the chimney center was picked manually from the base to the top of the pockmarks for all sequences (S1–S5). Picking was carried out on time slices extracted from 3-D seismic data as shown in the example presented in Figure 3c. Detailed pockmark analysis was limited to the two upper sequences [Sierro et al., 2009].

3. Obliquely Migrating Pockmark Distribution

In the B/H canyon interfluvial, 138 pockmarks with diameters ranging from 10 to 130 m were detected on the seafloor (Figure 1); all have the same morphology as those first documented in the literature [King and

movement of Messinian evaporite deposits affects the deeper sector of the margin. At the water depth of the study area and within the observed sediment ascribed to late Quaternary, the influence of faulting seems to be minor [Jouet, 2007]. Five seismo-stratigraphic sequences (S1 to S5) defined regionally [Bassetti et al., 2008 and references therein] are bounded by seismic reflectors Dnn. They are regional surfaces with an erosional expression on the shelf (stacked sequence boundaries and maximum flooding surfaces) and correlative conformities corresponding to maximum flooding surfaces (MFS) on the continental slope [Jouet, 2007]. On the slope, the MFS correspond to condensed sedimentary layers formed during periods of rising and high sea level, when sources of terrigenous sediment shifted landward. These layers are characterized by coarse-grained planktonic foraminifera and other sand-size particles. It is represented by a thin

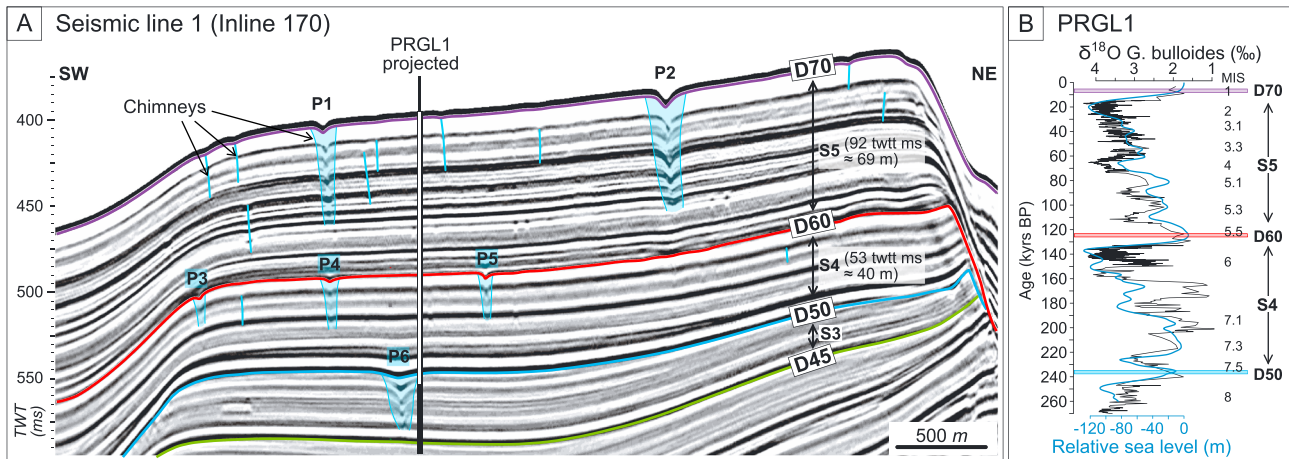


Figure 2. Pockmarks are present within distinct stratigraphic units. (a) Strike-oriented seismic line 1 (inline 170) from 3-D seismic data set, located in Figure 1b. Four maximum flooding surfaces (D70, D60, D50, and D45) are shown marking the highest sea level of the 100 kyr climatic cyclicity [Basetti et al., 2008; and references therein], clearly demonstrating that pockmark chimneys end in seismic discontinuities. P1 to P6 = pockmark numbers (as in Figure 1b). (b) Relationship between relative sea level [Waelbroeck et al., 2002] and multi-proxy analysis of PRGL1 [Sierra et al., 2009; Frigola et al., 2012]. Dated seismic reflectors D70, D60, and D50 identified in the Gulf of Lions are superimposed on the relative sea level and $\delta^{18}\text{O}$ curves and represent Marine Isotope Stages (MIS) 7, 5, and 1.

MacLean, 1970]. The pockmarks are mostly circular or oval in shape and have a conical or dish-shaped vertical section. All pockmarks and paleo-pockmarks disturb the major seismic surfaces D70, D60, and D50 (Figures 2a and 4). In other words, the pockmarks and their associated chimneys show marked segregation as they are present only within distinct stratigraphic units: 138 within sequence S5 and 168 within S4 (Figure 2). The distribution of pockmarks varies from one sequence to the next (Figures 2 and 4).

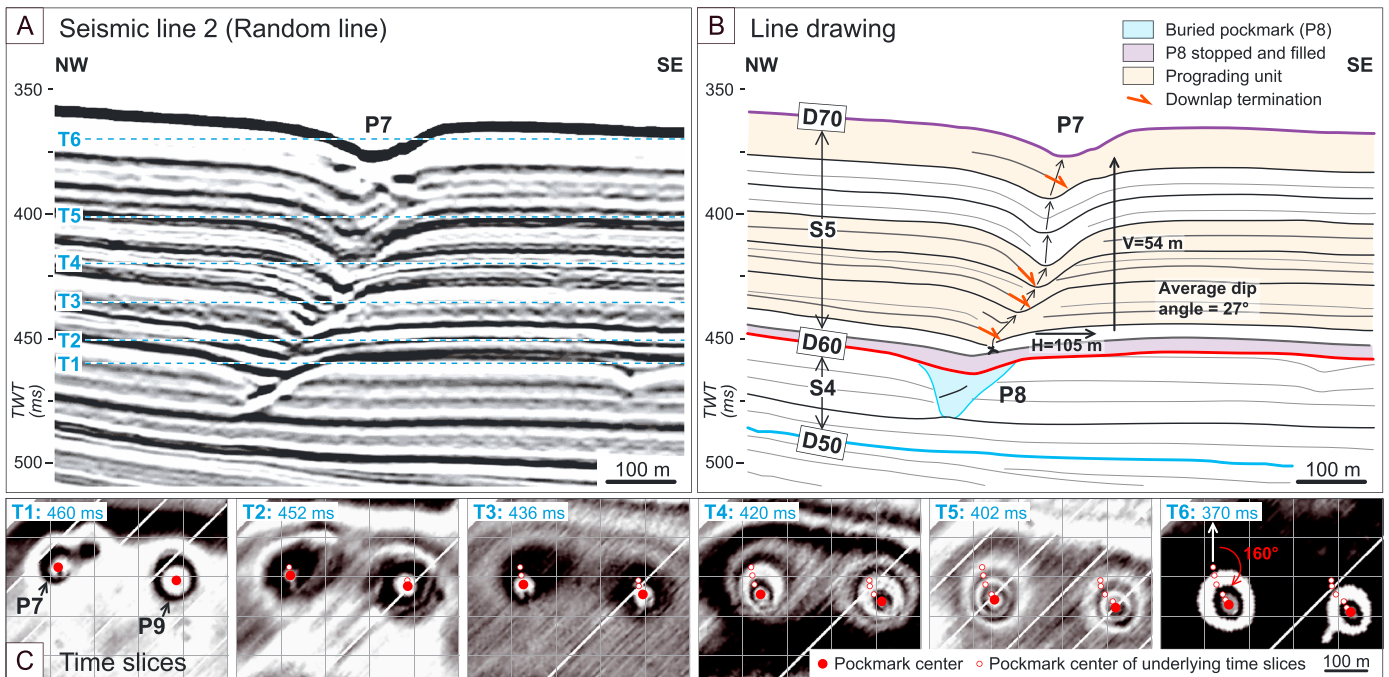


Figure 3. Evidence for oblique chimneys in the downslope direction. (a) Dip-oriented seismic line 2 from 3-D data set (location in Figure 1). Pockmark chimneys migrate obliquely with a horizontal offset toward the basin. (b) A pockmark originating in the sedimentary layer above D60 and terminating in D70, affecting the whole sequence. In detail, the stratigraphic organization shows downlap terminations in the center of the chimney and evidence for prograding stages. The average chimney dip angle (with respect to the horizontal) of this pockmark is 27°. (c) Time slices (location in Figure 1) revealing the migration of the pockmark center (in red).

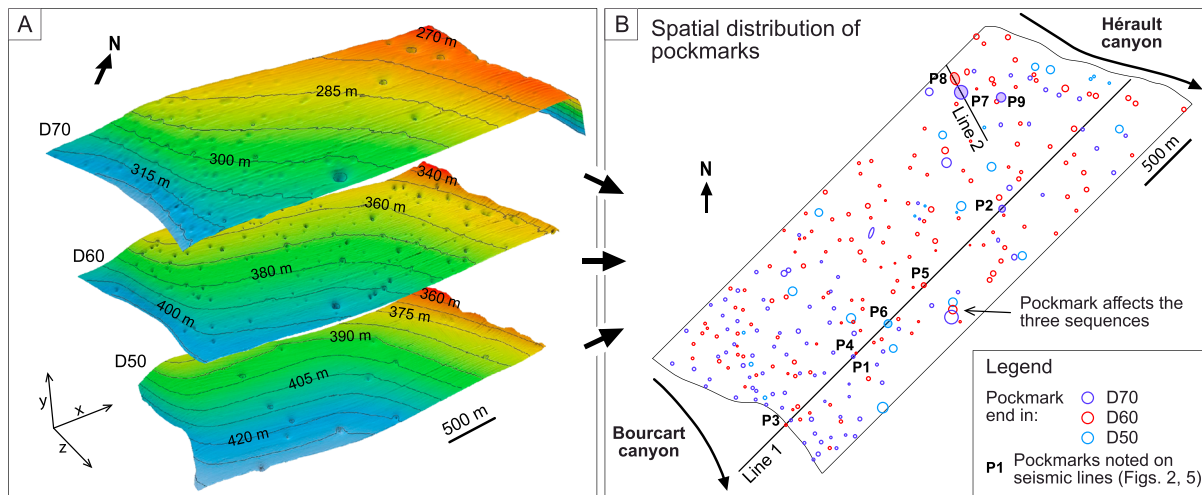


Figure 4. Pockmark distribution change from one sequence to the next. (a) Isochron maps of the three reflectors D70, D60, and D50, extracted from 3-D seismic data. Observation in three dimensions provides a better understanding of pockmark spatial arrangement. (b) Plan view of all the pockmarks observed in the three reflectors D70, D60, and D50. Pockmarks generally affect only one sequence, although some may affect two or three.

The track of the pockmarks through the sedimentary layers that are not disturbed by faulting was followed thanks to the obtained 3-D seismic data (Figure 4). Whereas the pockmark chimneys are vertical if observed in inline sections (Figure 2a), when crossed in the direction of the local slope they appear oblique (Figure 3). Oblique chimneys originate on a condensed layer, propagate along an entire sequence, and end up below the following condensed layer. Seismic reflections present downlap terminations within the chimney of the pockmark, corresponding to sediment progradation during the phase of pockmark development (Figure 3b). Progradation occurs down the maximum slope angle, e.g., the chimney of pockmark P7 is rooted in the condensed layer D60, affects the unit S5, and terminates below the condensed layer D70 (Figure 3).

The 138 pockmarks observed within sequence S5 are associated with oblique chimneys with an average dip angle of $23 \pm 4^\circ$ to the horizontal, while the 168 pockmark chimneys within sequence S4 exhibit an average dip angle of $43 \pm 4^\circ$. Thus, pockmark centers migrate sideways in the downslope direction at an angle of between 22° and 45° . The pockmarks show an excellent linear relationship between horizontal and vertical migration: on average, pockmarks with the largest vertical extent (V) also exhibit maximum lateral displacement (H) (Figure 3b). By comparing the two sets of pockmarks in sequences S5 and S4, we can observe that pockmarks grow vertically with a more oblique trajectory within sequence S5, which is locally thicker than S4 and has a sediment accumulation rate 1.7 times higher. In plan view, the azimuth of chimney migrations lies between 158°N and 226°N within S5, and between 160°N and 230°N within S4 (Figure 3c). Pockmark migration azimuth is thus influenced by local slope, with a deviation of around 20° to the west.

4. Discussion

The segregation of pockmarks and associated chimneys into discrete stratigraphic intervals—the expression of sea level variations related to 100 kyr Milankovitch climatic cycles—is a key procedure required to address the issue of their formation. This procedure also demonstrates the role of changes in water column thickness observed via the hydrostatic pressure response on the gas seeps. However, the latter process can have an impact only if the fluid contains gas. The ideal environment for the formation of biogenic methane is one containing areas of rapidly accumulating, fine-grained muddy sediments rich in organic matter [Rice and Claypool, 1981; Hovland et al., 1993], such as those observed in the study area during sea level falls (Figure 5b). The sediment accumulated during lowstands is characterized by high organic matter content, with total organic carbon (TOC) levels likely comparable to those presently measured off the Rhône prodelta [García-García et al., 2006] (TOC between 1 and 2% wt). Such organic matter concentrations are sufficient to allow significant biogenic gas generation [Jané et al., 2010], with the TOC concentrations comparable to those documented in the Congo Basin [Andresen and Huuse, 2011] and in the South China Sea [Sun et al., 2012], resulting in the widespread formation of pockmarks [Hovland and Judd, 1988]. Although the exact amount of

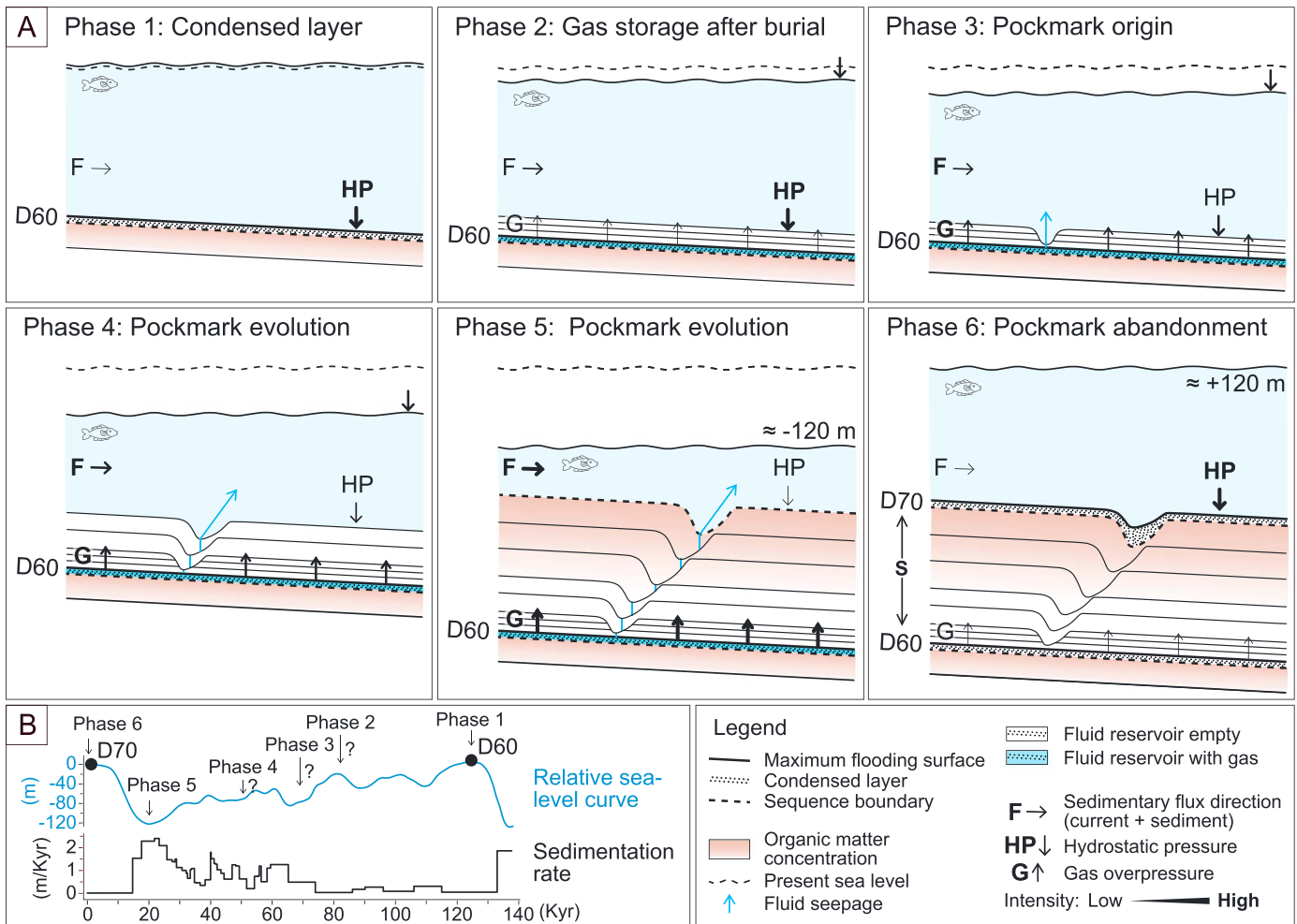


Figure 5. Comprehensive view of the formation of obliquely migrating pockmarks. (a) Six sketches illustrating the phases of the idealized scenario leading to the formation of oblique pockmarks under the control of relative sea level changes. See text for details. (b) Sea level variations [Waelbroeck et al., 2002] and sedimentation rate [Sierra et al., 2009] at site PRGL1 for the last sequence S5 (MIS 5 to MIS 1), together with the timing of pockmark activity phases numbered 1 to 6.

gas needed to form pockmarks of a given size is not known, biogenically produced methane pools make an important contribution to pockmark formation, particularly for pockmarks without deeply rooted feeder systems, as observed in shallow sequences of the Gulf of Lions. Here gas migrated into the condensed sedimentary layers where it was then stored. Indeed, when draped by less permeable layers, condensed layers act as good transient fluid reservoirs, as previously seen by Riboulot et al. [2013] in the Niger submarine delta.

The downlap termination of seismic reflections within chimneys demonstrates the syn-sedimentary evolution of fluid seepages. The coupled observation of the oblique vertical migration of the chimneys and the progradation of sediment within pockmarks in the direction of the local slope reveals a long-lasting, syn-sedimentary process of pockmark growth, characterized by sediment deposition/progradation on the updip side and erosion on the downdip side. Gas plumes in the water column are laterally deflected in the direction of the dominant bottom current [Rollet et al., 2006; Leifer and Judd, 2002]. Bottom currents and gas plumes actively participate in modifying pockmark shape by creating elongated pockmarks [Dandapath et al., 2010]. These two local factors explain the observed erosion of pockmark downdip sides. In summary, the oblique pockmark growth reflects a sediment flux from the continental margin following the local slope, with a western component aligned with the dominant flow direction of the Liguro-Provençal Current [Millot, 1990]. A few pockmarks have formed over paleo-pockmarks (Figure 4). The chimneys form a high-permeable zone, analogous to what is known as a “seal bypass system” [Cartwright et al., 2007], in

which fluids and gas can be transported faster than would otherwise be allowed by normal permeability levels in the sediment pore network. High fluid overpressure opening a hydro fracture through low-permeable sediments is a common first phase in all of these bypass structures [Arntsen *et al.*, 2007; Cartwright *et al.*, 2007; Løseth *et al.*, 2009; Rodrigues *et al.*, 2009].

Although the increase in sediment accumulation rate observed between the two sequences studied here is a cause of overpressure in more porous layers, in most cases the generated overpressure is not sufficient to induce hydrofracturing in the overburden and initiate focused fluid flow [Talukder, 2012]. Indeed, the role of sedimentation rate in pockmark morphology has been revealed in Belfast Bay where Brothers *et al.* [2012] found that the largest pockmarks occur where Holocene sediment is thickest. Seismicity and faulting can cause an overpressure to initiate gas seeps but, as presented previously, the study area is relatively stable, not disturbed by faults, and shows very low seismic activity. Other factors such as surface conditions, eustatic sea level, and ocean bottom water temperatures are also suspected to affect gas seeps [Judd *et al.*, 2002]. Sea level falls cause a reduction in hydrostatic pore pressure that has an impact on gas solubility, a decrease that can cause gas exsolution. The exsolved gas then accumulates in relatively more porous layers interbedded within less permeable layers [Lafuerza *et al.*, 2009], inducing hydrofracture in the overburden and the creation of post-sedimentary pockmarks. Sea level fall is the most efficient trigger mechanism for pockmark formation in the B/H canyon interfluvium, as already suggested for the Lower Congo Basin [Andresen and Huuse, 2011] and the Nyegga region of offshore Norway [Plaza-Faverola *et al.*, 2011]. Such a process is also strongly proposed for the Niger submarine delta, where Riboulot *et al.* [2013] have revealed pockmarks to be present only within distinct stratigraphic sequences. Conversely, the increased pockmark activity recorded during periods of global sea level falls represents an overlooked mechanism possibly responsible for the injection of large quantities of gas into the ocean and the atmosphere at the end of glaciations. Judd *et al.* [2002] have previously argued that geological sources of gas and reservoirs influence the direction and speed of global climate change and constrain extremes of climate. However, whether emitted seafloor methane reaches the atmosphere is debatable. In fact, 10% of gas emissions at the seafloor are lost to dissolution for a typical low-flux bubble plume [Leifer *et al.*, 2006]. Fluxes of the greenhouse gas methane from marine geological sources to the atmosphere may be significant, but they are as yet poorly quantified [Solomon *et al.*, 2009]. Dickens [2003] has proposed that sudden deep ocean warming and subsequent gas hydrate dissociation could result in large amounts of methane being released into the ocean, thus contributing to atmospheric warming.

5. Conceptual Model of Oblique Pockmark Development

A scenario composed of six phases could explain the origin, evolution, and abandonment of a pockmark related to 100 kyr sea level changes (Figure 5). When the sea level rises and reaches the highstand (Phase 1), a condensed sediment unit forms along the slope above the sequence boundary and the underlying prodeltaic sediments deposited during the previous lowstand. After burial under fine-grained "offshore" clays during sea level fall resumes, the coarse-grained condensed interval becomes a potential fluid reservoir. Biogenic gases produced within the underlying prodeltaic sediment layers are accumulated in the condensed section (Phase 2). During sea level fall, hydrostatic pressure in the fluid reservoir decreases, creating an exsolution of gas, and pockmarks are created [Lafuerza *et al.*, 2009; Riboulot *et al.*, 2013 and references therein] (Phase 3). Pockmark evolution then becomes syn-sedimentary. Sediment should fill pockmark depressions, but fluid seepage hampers the filling. The interaction of fluid seepage and bottom current favors the lateral deflection of the gas plume in the water column along the dominant current direction [Leifer and Judd, 2002; Rollet *et al.*, 2006]. This causes differential erosion/deposition on pockmark flanks, with downstream flanks eroded while sediment progrades from upstream flanks (Phases 4 and 5). Pockmark migration is possible only if fluid seepage occurs. Finally, when the sea level rises, hydrostatic pressure in the reservoir increases and fluid expulsion decreases. On the upper slope, the sedimentation rate decreases (condensation) in association with the landward shift of fluvial outlets. Phase 6 corresponds to pockmark abandonment. The migration of pockmarks ceases, with sediment filling the pockmarks during the onset of the next sea level fall.

6. Conclusion

The present Gulf of Lions integrated study has provided evidence for hundreds of pockmarks and their associated oblique chimneys, confined stratigraphically with syn-sedimentary development in association

with eustatic cycles, with a model of pockmark formation explaining the origin, evolution, and abandonment of oblique pockmarks. The stratigraphic control on pockmark distribution within sequences is indirect evidence that fluid seeps function, at least in our study area, in response to glacio-eustatic fluctuations driven by 100 kyr Milankovitch cycles. We suggest that the water column loss occurring during sea level lowstands (ca. 120 m during the last glaciation) enhances massive expulsion of biogenic gas into the ocean, thus may contribute to atmospheric warming which is dependent on the proportion of methane retained in water column.

Acknowledgments

We thank B. Marsset, S. Jorry, and A. Chalm for reviewing the manuscript and providing insightful comments. B. Marsset is also acknowledged for the acquisition and processing of the 3-D HR seismic data. The captains and crews of "Le Suroit" are acknowledged for their assistance provided during the cruise "Calimero". P. Imbert, E. Cauquil, L. Loncke, and M. Voisset contributed to lively discussions on the origin of pockmarks.

The Editor thanks two anonymous reviewers for their assistance in evaluating this paper.

References

- Agirrezabala, L. M., S. Kiel, M. Blumenberg, N. Schäfer, and J. Reitner (2013), Outcrop analogues of pockmarks and associated methane-seep carbonates: A case study from Lower Cretaceous (Albian) of the Basque-Cantabrian Basin, western Pyrenees, *Palaeogeogr. Palaeoclimatol. Palaeoecol.*, *390*, 94–115.
- Andresen, K. J., and M. Huuse (2011), Bulls-eye' pockmarks and polygonal faulting in the Lower Congo Basin: Relative timing and implications for fluid expulsion during shallow burial, *Mar. Geol.*, *279*, 111–127, doi:10.1016/j.margeo.2010.10.016.
- Andresen, K. J., M. Huuse, and O. R. Clausen (2008), Morphology and distribution of Oligocene and Miocene pockmarks in the Danish North Sea - Implications for bottom current activity and fluid migration, *Basin Res.*, *20*, 445–466.
- Arntsen, B., L. Wensaas, H. Loseth, and C. Hermanrud (2007), Seismic modeling of gas chimneys, *Geophysics*, *72*(5), 251–259.
- Bassetti, M. A., S. Berne, G. Jouet, M. Taviani, B. Dennielou, J. A. Flores, A. Gaillot, R. Gelfort, S. Lafuerza, and N. Sultan (2008), The 100-ka and rapid sea level changes recorded by prograding shelf sand bodies in the Gulf of Lions (western Mediterranean Sea), *Geochem. Geophys. Geosyst.*, *9*, Q11R05, doi:10.1029/2007GC001854.
- Boe, R., L. Rise, and D. Ottesen (1998), Elongate depressions on the southern slope of the Norwegian Trench (Skagerrak): Morphology and evolution, *Mar. Geol.*, *146*, 191–203.
- Brothers, L. L., J. T. Kelley, D. F. Belknap, W. A. Barnhardt, B. D. Andrews, C. Legere, and J. E. H. Clarke (2012), Shallow stratigraphic control on pockmarks distribution in north temperate estuaries, *Mar. Geol.*, *329–331*, 34–45.
- Cartwright, J., M. Huuse, and A. Aplin (2007), Seal bypass system, *AAPG Bull.*, *91*, 1141–1166.
- Cathles, L. M., Z. Su, and D. Chen (2010), The physics of gas chimney and pockmark formation, with implications for assessment of seafloor hazards and gas sequestration, *Mar. Pet. Geol.*, *27*, 82–91.
- Dandapath, S., B. Chakraborty, S. M. Karisiddaiah, A. Menezes, G. Ranade, W. Fernandes, D. K. Naik, and K. N. Prudhvi Raju (2010), Morphology of pockmarks along the western continental margin of India: Employing multibeam bathymetry and backscatter data, *Mar. Pet. Geol.*, *27*, 2107–2117.
- Dickens, G. R. (2003), Rethinking the global carbon cycle with a large, dynamic and microbially mediated gas hydrate capacitor, *Earth Planet. Sci. Lett.*, *213*, 169–183.
- Frigola, J., et al. (2012), A 500 kyr record of global sea-level oscillations in the Gulf of Lion, Mediterranean Sea: New insights into MIS 3 sea-level variability, *Clim. Past*, *8*, 1067–1077, doi:10.5194/cp-8-1067-2012.
- García-García, A., D. Orange, T. Lorenson, O. Radakovitch, T. Tesi, S. Miserocchi, S. Berné, P. L. Friend, C. Nittrouer, and A. Normand (2006), Shallow gas off the Rhône prodelta, Gulf of Lions, *Mar. Geol.*, *234*, 215–231.
- Gay, A. (2002), Les marqueurs géologiques de la migration et de l'expulsion des fluides sédimentaires sur le plancher des marges passives matures. Exemples dans le Bassin du Congo, Thèse Université de Lille 1, 426 pp.
- Hammer, O., and K. E. Webb (2010), Piston coring of Inner Oslo fjord Pockmarks, Norway: constraints on age and mechanism, *Nor. J. Geol.*, *90*, 79–91.
- Hovland, M. (1987), The formation of pockmarks and their potential influence on offshore construction, *Proc. JSCSE*, *388*(III-8), 13–22.
- Hovland, M., and A. G. Judd (1988), *Seabed Pockmarks and Seepages*, 293 pp., Graham and Trotman, London.
- Hovland, M., A. G. Judd, and L. H. King (1984), Characteristic features of pockmarks on the north sea floor and scotian shelf, *Sedimentology*, *31*, 471–480.
- Hovland, M., A. G. Judd, and R. A. Burke Jr. (1993), The global flux of methane from shallow submarine sediments, *Chemosphere*, *26*, 559–578.
- Hustoft, S., J. Mienert, S. Bünz, and H. Nouzé (2007), High-resolution 3D-seismic data indicate focused fluid migration pathways above polygonal fault systems of the mid-Norwegian margin, *Mar. Geol.*, *245*, 89–106.
- Jané, G., A. Maestro, G. Ercilla, J. López-Martínez, J. R. De Andrés, D. Casas, D. González-Aller, and M. Catalán-Morollón (2010), Occurrence of pockmarks on the Ortegale Spur continental margin, Northwestern Iberian Peninsula, *Mar. Pet. Geol.*, *27*, 1551–1564.
- Josenhans, H. W., L. H. King, and G. B. Fader (1978), A side-scan sonar mosaic of pockmarks on the Scotian shelf, *Can. J. Earth Sci.*, *15*, 831–840.
- Jouet, G. (2007), Enregistrements stratigraphiques des cycles climatiques et glacio-eustatiques du Quaternaire terminal. Modélisations de la marge continentale du Golfe du Lion, Thèse Université Bretagne Occidentale, vol. 1, 443 pp.
- Judd, A. G., M. Hovland, L. I. Dimitrov, S. Garca Gil, and V. Jukes (2002), The geological methane budget at continental margins and its influence on climate change, *Geofluids*, *2*, 109–126.
- King, L. H., and B. MacLean (1970), Pockmarks on the Scotian shelf, *Geol. Soc. Am. Bull.*, *81*, 3141–3148.
- Lafuerza, S., N. Sultan, M. Canals, J. Frigola, S. Berné, G. Jouet, M. Galavazi, and F. J. Sierro (2009), Overpressure within upper continental slope sediments from CPTU data, Gulf of Lion, NW Mediterranean Sea, *Int. J. Earth Sci.*, *98*(4), 751–768, doi:10.1007/s00531-008-0376-2.
- Leifer, I., and A. G. Judd (2002), Oceanic methane layers: The hydrocarbon seep bubble deposition hypothesis, *Terra Nova*, *14*, 417–424.
- Leifer, I., B. P. Luyendyk, J. Boles, and J. F. Clark (2006), Natural marine seepage blowout: contribution to atmospheric methane, *Global Biogeochem. Cycles*, *20*, GB3008, doi:10.1029/2005GB002668.
- Løseth, H., M. Gading, and L. Wensaas (2009), Hydrocarbon leakage interpreted on seismic data, *Mar. Pet. Geol.*, *26*, 1304–1319.
- Millot, C. (1990), The gulf of Lions' hydrodynamics, *Cont. Shelf Res.*, *10*, 885–894.
- Moss, J., and J. A. Cartwright (2010), 3D seismic expression of km-scale fluid escape pipes from offshore Namibia, *Basin Res.*, *22*, 481–501, doi:10.1111/j.1365-2117.2010.00461.x.
- Nocquet, J. M. (2012), Present-day kinematics of the Mediterranean: A comprehensive overview of GPS results, *Tectonophysics*, *579*, 220–242.
- Plaza-Faverola, A., S. Bünz, and J. Mienert (2011), Repeated fluid expulsion through sub-seabed chimneys offshore Norway in response to glacial cycles, *Earth Planet. Sci. Lett.*, *305*, 297–308, doi:10.1016/j.epsl.2011.03.001.
- Riboulot, V., A. Cattaneo, N. Sultan, S. Garziglia, S. Ker, P. Imbert, and M. Voisset (2013), Sea-level change and free gas occurrence influencing a submarine landslide and pockmark formation and distribution in deepwater Nigeria, *Earth Planet. Sci. Lett.*, *375*, 78–91.

- Rice, D. D., and G. E. Claypool (1981), Generation, accumulation and resource potential of biogenic gas, *AAPG Bull.*, *65*, 5–25.
- Rodrigues, N., P. R. Cobbold, and H. Løseth (2009), Physical modelling of sand injectites, *Tectonophysics*, *474*, 610–632.
- Rollet, N., G. A. Logan, J. M. Kennard, P. E. O'Brien, A. T. Jones, and M. Sexton (2006), Characterisation and correlation of active hydrocarbon seepage using geophysical data sets: an example from the tropical, carbonate Yampi Shelf, Northwest Australia, *Mar. Pet. Geol.*, *23*, 145–164.
- Sierro, F. J., et al. (2009), Phase relationship between sea level and abrupt climate change, *Quat. Sci. Rev.*, *28*, 2867–2881.
- Solomon, E., M. Kastner, I. R. MacDonald, and I. Leifer (2009), Considerable methane fluxes to the atmosphere from hydrocarbon seeps in the Gulf of Mexico, *Nat. Geosci.*, *2*, 561–565.
- Sun, Q., S. Wu, J. Cartwright, and D. Dong (2012), Shallow gas and focused fluid flow systems in the Pearl River Mouth Basin, northern South China Sea, *Mar. Geol.*, *315-318*, 1–14, doi:10.1016/j.margeo.2012.05.003.
- Talukder, A. R. (2012), Review of submarine cold seep plumbing systems: Leakage to seepage and venting, *Terra Nova*, *24*, 255–272, doi:10.1111/j.1365-3121.2012.01066.x.
- Thomas, Y., B. Marsset, G. K. Westbrook, C. Grall, L. Geli, P. Henri, G. Cifçi, A. Rochat, and H. Saritas (2012), Contribution of high-resolution 3D seismic near-seafloor imaging to reservoir-scale studies: Application to the active North Anatolian Fault, Sea of Marmara, *Near Surf. Geophys.*, *10(4)*, 291–300, doi:10.3997/1873-0604.2012019.
- Waelbroeck, C., L. D. Labeyrie, E. Michel, J.-C. Duplessy, J. McManus, K. Lambeck, E. Balbon, and M. Labracherie (2002), Sea level and deep water changes derived from benthic foraminifera isotopic record, *Quat. Sci. Rev.*, *21*, 295–305.